

Inhibitive Assessment of N-(8-Bromo-3H-Phenoxazin-3-Ylidene)-N, N'-Dimethylaminium, as A Novel Corrosion Inhibitor for Mild Steel In 1.0 M Hcl

M. Bozorg^a, T. Shahrabi Farahani^{a,*}, Gh. Mohammadi Ziarani^b, J. Neshati^c, Z. Chaghazardi^a, P. Gholamzade^b, F. Ektefa^d

^a Department of Materials Engineering, Faculty of Engineering, Tarbiat Modares University, Tehran, Iran.

^b Department of Chemistry, Alzahra University, Tehran, Iran.

^c Research Institute of Petroleum Industry, RIPI, Tehran, Iran.

^d Department of Chemistry, Faculty of Science, Tarbiat Modares University, Tehran, Iran.

ARTICLE INFO

Article history:

Received 19 Apr. 2014

Accepted 21 May 2014

Available online 31 Aug. 2014

Keywords:

Corrosion
Inhibitor
Mild steel
DPhDMA
EIS

ABSTRACT

The inhibition effect of N-(8-bromo-3H-phenoxazin-3-ylidene)-N,N'-dimethylaminium (DPhDMA) on the corrosion behavior of mild steel in 1.0 M HCl solution has been studied. Weight loss measurements, potentiodynamic polarization, electrochemical impedance spectroscopy (EIS) and quantum chemical calculations were performed in this study. Electrochemical results revealed that DPhDMA is an effective mixed type inhibitor for mild steel in 1.0 M HCl solution, and its inhibition efficiency increased with increasing its concentration and with the immersion time of the samples in the corrosive media. The adsorption of DPhDMA also led to a reduction in electric double layer capacitance and an increase in charge transfer resistance confirming its inhibitive effect on the corrosion behavior of the mild steel samples. The thermodynamic parameters governing the adsorption process showed that DPhDMA was adsorbed spontaneously on mild steel surface through a combination of physical and chemical mechanisms following Langmuir adsorption isotherm. Quantum chemical calculations were used to correlate the performance of DPhDMA with its electronic structural parameters.

1. Introduction

Acid pickling is a descaling process used for removing undesired scale, rust or other corrosion products from the surface of equipments such as boilers, heat exchangers, cooling towers, etc.[1–3]. Acidic solutions used in acid pickling processes may impart severe damages to the metallic substrate and cause excess acid consumption due to corrosion,

which is a problem of practical significance in industrial environments. Among various techniques proposed to diminish the unexpected destructive effect of acid pickling processes, the addition of inhibitor is the most practical and affordable method [4–7].

Many studies have reported the application of organic inhibitors, which are usually heterocyclic compounds containing

Corresponding author:

E-mail address: tshahrabi34@modares.ac.ir (Taghi Shahrabi Farahani).

heteroatoms such as Oxygen, Nitrogen, Sulfur, etc., as an effective method for protecting metals against acidic corrosion [8–11]. These compounds inhibit the corrosion of metals through the formation of a protective film on the metal surface, which acts as a barrier that impedes the charge transfer from the metal to the corrosive solution and vice versa [12–14]. Therefore, the inhibition efficiency of organic inhibitors depends highly on the number of active adsorption sites, adsorption mode, charge density at hetero atoms and geometry, planarity, and size of the inhibitor molecules [15–18].

It has also been observed that the presence of aromatic cycles, π electrons and multiple bonds that act as adsorption centers along with heteroatoms can improve the corrosion inhibition efficiency of such organic compounds [19–22].

This study deals with investigating the inhibition effect of a new synthesized inhibitor, N-(8-bromo-3H-phenoxazin-3-ylidene)-N, N'-dimethylaminium (DPhDMA), on the corrosion behavior of mild steel in 1.0 M HCl solution. The study was carried out using electrochemical impedance spectroscopy and potentiodynamic polarization tests and computational methods to survey the inhibition mechanism.

2. Experimental

2. 1. Materials

2. 1. 1. Synthesis of DPhDMA

In a round bottom flask, N, N'-dimethylaniline **1** (2 ml) was dissolved in diluted HCl and placed in an iced-salt bath. The temperature was fixed between 0-3 °C. A solution of NaNO₂ (1.5 gr) in water was slowly poured into the mixture. In this condition, the mixture color changed to dark orange. After completion of the reaction, NaOH solution added to the mixture until it became green and alkaline [23]. The solid, which is N, N-dimethylaniline **2**, was filtered and dried in the next step. Following the DPhDMA **4** synthesis, *p*-bromophenol **3** (10 mmol), and AlCl₃ (10 mmol) were added into a solution of *p*-nitroso-N, N-dimethylaniline **2** (10 mmol) in ethanol, and the mixture was heated at 70 °C for 12 h (fig. 1).

The color of the solution changed from green to dark blue. After completion of the reaction, the mixture was filtered and washed with EtOAc to remove the remained **2** and then dried for analyzing the pure product. ¹H NMR (D₂O, 400 MHz): δ_{H} (ppm)= 3 (6H, s, NCH₃), 6.7 (2H, arom), 6.83 (1H, dd, arom), 7.17 (1H, d, arom), 7.26 (1H, d, arom) and 7.4 (1H, arom). FT-IR (KBr): ν_{max} = 1512-1620 (aromatic ring vibration), 1319 (C-N vibration), 600 (C-Br vibration). The FTIR and 1H NMR spectra of the DPhDMA are showed in Fig 2 and Fig 3, respectively.

2. 1. 2. Specimens and test solution preparation

Experiments were carried out using mild specimen with the following composition: 0.18% Cu, 0.085% C, 0.04% Si, 1.02% Mn, 0.054% P, 0.33% S, 0.06% Cr, 0.11% Ni, 0.29% Pb and the remainder iron. The mild steel surface was abraded with emery papers (grades 80, 120, 240, 320, 400, 600, 800, 1000), polished to a near mirror finish by a polishing cloth with water based liquid solution of 0.5 μm alumina, washed with distilled water, degreased with acetone and finally dried with a cold air stream. The aggressive solution of 1.0 M HCl was prepared by diluting 37% analytical grade HCl (Merck) by distilled water. The concentration range of the used DPhDMA was 25-100ppm and a blank solution without DPhDMA was taken as the witness solution for comparison. The test solutions were opened to the atmosphere and the temperature was controlled. Also, for each experiment a freshly prepared solution was used.

2. 2. Methods

2. 2. 1. Weight loss measurements

Weight loss tests were performed on mild steel coupons after 24 h exposure to 1.0 M HCl solution containing various concentrations of DPhDMA (0-100 ppm). In order to investigate the effect of immersion time of the samples in the inhibited solution on inhibition efficiency, weight loss tests were also carried out on mild steel samples after different immersion times (24-96h) in 1.0 M HCl solution containing 0, 50, and 100 ppm of DPhDMA.

Mild steel specimens with 3 cm length, 1.5 cm width, and 0.3 cm thickness were pretreated

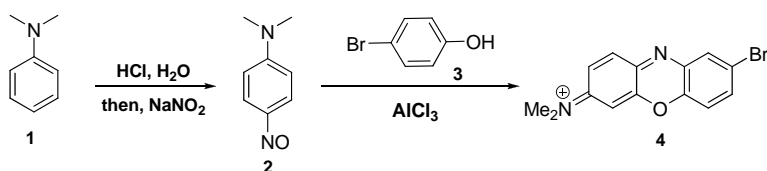


Fig. 1. Synthesis of DPhDMA

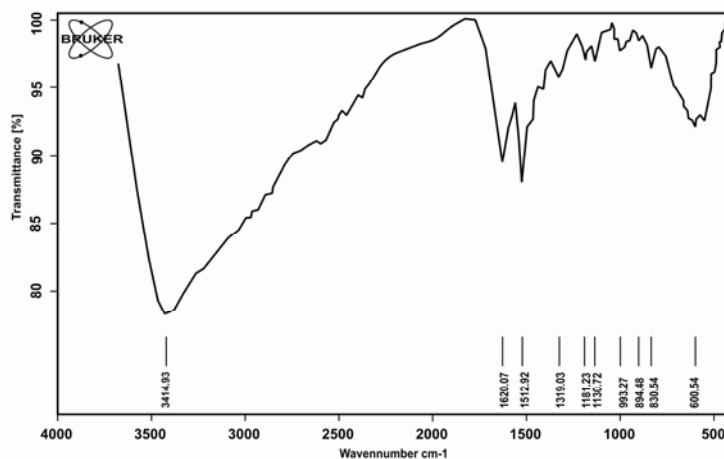


Fig. 2. FT-IR spectrum of DPhDMA

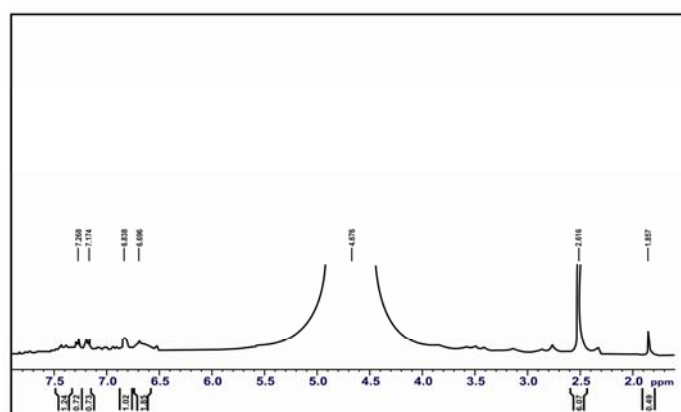


Fig. 3. ^1H NMR spectrum of DPhDMA

as previously described and weighed before immersion in the corrosive media. After suspension for the desired period of time in the aggressive solution, the specimens were removed, washed, dried and then the weight loss was measured by the analytic balance.

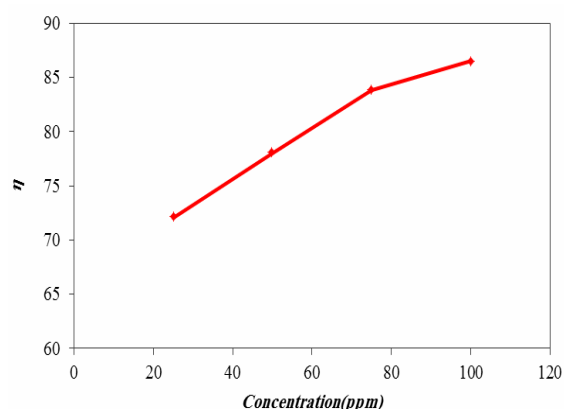
2. 2. 2. Electrochemical studies

Electrochemical tests were carried out on mild steel in HCl solution containing 0-100 ppm of DPhDMA using a conventional three electrode electrochemical cell and an Autolab potentiostat/galvanostat (model 302N, Netherlands) and a personal computer equipped

with Nova1.7 software. Mild steel specimens were used as the working electrode (WE), platinum as the counter electrode (CE) and saturated calomel electrode (SCE), separated from the cell by a glass frit, as the reference electrode (RE). All the reported potentials in this paper were measured with respect to the SCE. Electrochemical impedance spectroscopy (EIS) was conducted at open circuit potential after 1 h of immersion in the frequency range of 100 kHz to 0.1 Hz by a sine wave with a potential perturbation amplitude of 5 mV. Corrosion rates were also obtained by Tafel technique. Potentiodynamic polarization curves

Table 1. Weight loss results for samples immersed in 1.0 M HCl with and without different concentrations of the synthesized inhibitor

Concentration of inhibitor (ppm)	Corrosion Rate (mpy)	θ	η (%)
0	92.4	-	-
25	25.8	0.720	72.0
50	20.3	0.780	78.0
75	14.9	0.838	83.8
100	12.4	0.865	86.5

**Fig. 4.** Variation of the inhibition efficiency of steel after immersion in 1.0M HCl containing different concentrations of the DPhDMA

were recorded from -250mV to +250mV around the open circuit potential with a sweep rate of 1mV/s. 2.2.3. Quantum chemical calculations The molecular structure of DPhDMA molecules were optimized by the Becke3-Lee-Yang-Parr (B3LYP) exchange-correlation functional in conjugation with 6-31G** basis set for all atoms without any symmetry constraints. All quantum chemical calculations were performed by means of Gaussian 98 program package. Quantum chemical parameters such as the energy of the Highest Occupied Molecular Orbital (E_{HOMO}), the energy of the Lowest Unoccupied Molecular Orbital (E_{LUMO}), the energy gap between these orbitals ($\Delta E = E_{HOMO} - E_{LUMO}$), and the dipole moment (μ) were calculated.

3. Results and Discussion

3.1. Weight loss measurements

In order to investigate the effect of the inhibitor concentration on the inhibition efficiency of the inhibitor under consideration, weight loss tests

were carried out after suspension of mild steel samples in 1.0 M HCl solution containing various concentrations of DPhDMA (25-100 ppm) for 24 h. The obtained results are presented in Table 1 and Fig 4.

The values for corrosion rate, surface coverage and inhibition efficiency were calculated as follows [21]:

$$C.R.(mpy) = \frac{534\Delta W}{D.A.t} \quad [1]$$

$$\theta = \frac{W_{uninh} - W_{inh}}{W_{uninh}} \quad [2]$$

$$\eta_w = \left(\frac{W_{uninh} - W_{inh}}{W_{uninh}} \right) \times 100 \quad [3]$$

Where θ is surface coverage, ΔW is the change in the weight of samples (mg), A is the exposed area of the samples (in^2), D is the metal's density (gr/cm^3), t is the immersion time (h), η is inhibition efficiency and W_{uninh} and W_{inh} are the weight changes (mg) of steel samples in the absence and presence of inhibitor, respectively.

It is obvious from both Fig. 4 and Table 1 that the inhibition efficiency reaches 86.5% upon the elevation in the concentration of DPhDMA to 100 ppm in 1.0 M HCl solution. Also, the corrosion rate of mild steel decreases from 92.4 mpy in the blank solution to 12.4 mpy in the solution containing 100 ppm of DPhDMA. This behavior might be due to the fact that organic compounds inhibit the corrosion of the metal through adsorption on its surface; therefore, higher concentration of inhibitor in the solution means higher surface coverage and hence stronger inhibitive action.

3.2. Electrochemical impedance spectroscopy

Nyquist plots of the mild steel specimens obtained in 1.0 M HCl solution containing

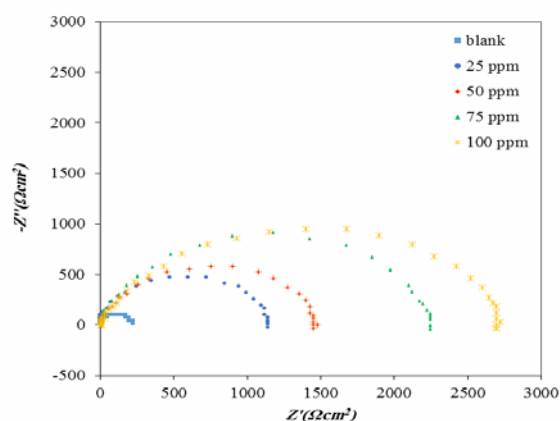


Fig. 5. Nyquist plots obtained for mild steel samples in 1.0M HCl with different concentrations of DPhDMA

various concentrations of the inhibitor under debate are illustrated in Fig. 5. Semicircular Nyquist curves shown in the figure are considered as single capacitive loops demonstrating the charge transfer controlled nature of the mild steel corrosion. Furthermore, the Nyquist curves are slightly depressed. Frequency dispersion caused by surface inhomogeneities might be the cause of the observed deviation from the ideal capacitive behavior. Noticeably, the shape of the Nyquist curves are preserved throughout all the tests, showing that the addition of this compound to 1.0 M HCl solution does not alter the mechanism of mild steel corrosion. It is clear that the addition of this compound to the corrosive solution causes the diameters of Nyquist curves to increase which is indicative of the increase in the impedance of mild steel surface and therefore the decrease in corrosion rates of mild steel specimens as a result of the inhibitive action of this compound.

In order to perform a detailed analysis of the inhibitive performance of this compound, EIS results were simulated using an equivalent electric circuit shown in Fig. 6, and chemical and physical properties of the system under consideration were calculated. In this Figure, R_s is the solution resistance, R_p is the polarization resistance and CPE is a constant phase element representing the electric double layer capacitance influenced by surface inhomogeneities implying the quasi capacitive behavior of the adsorbed ions in electric double

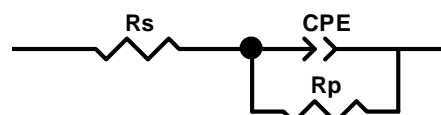


Fig. 6. Electrical equivalent circuit used to model metal/solution interface

layer and is calculated as follows [24, 25]:

$$CPE = Y_0 (\omega)^{n-1} \quad [4]$$

Where Y_0 is the CPE constant, ω is the angular frequency and n is the deviation parameter of the CPE: $-1 \leq n \leq 1$ where $n=1$ indicates ideal capacitive behavior of CPE element. Electrochemical parameters deduced through the fitting of EIS curves are summarized in Table 2.

Here the inhibition efficiency is calculated using the following equation:

$$\eta = \left(1 - \frac{R_p}{R_{p,inh}}\right) \times 100 \quad [5]$$

Where R_p is the polarization resistance in the absence of inhibitor and $R_{p,inh}$ is the polarization resistance in the presence of inhibitor. Moreover, the electric double layer capacity is calculated as follows [26, 27]:

$$C = \frac{K \epsilon_0 A}{d} \quad [6]$$

Where C is the capacity of the electric double layer, K is the dielectric coefficient, A is the area of capacitance planes, d is the distance between capacitance planes, and ϵ_0 is the vacuum permeability coefficient. Also presented in Table 2 are the values for Chi square (χ^2) which is the square of the standard deviation between the simulation and the real data. Chi square values near zero denote a good fitting [28, 29].

According to Table 2, the value of polarization resistance increases from 222 Ωcm^2 to 2680 Ωcm^2 , while the capacitance of the electric double layer decreases from 59.4 μFcm^{-2} to 33.0 μFcm^{-2} upon the addition of this compound to 1.0 M HCl blank solution and increasing its concentration to 100 ppm.

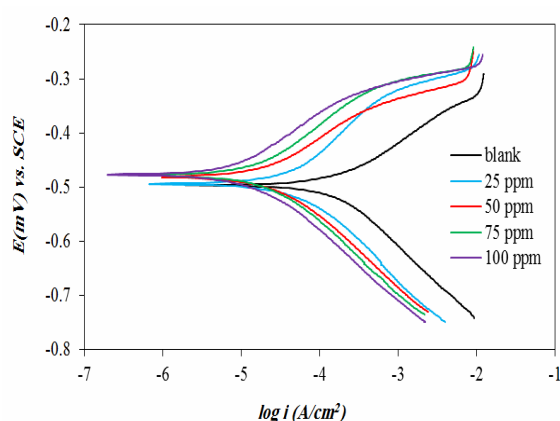
It can be concluded that the inhibitor performs through adsorption on the surface and formation of an electrical double layer, limiting the access of corrosive media to the metal surface, causing the polarization resistance to elevate and corrosion rates to decrease. Also,

Table 2. EIS parameters for the corrosion of aluminum in 1.0M HCl containing DPhDMA

<i>C</i> (ppm)	<i>R_p</i> (Ωcm ²)	<i>CPE-T</i> (μFcm ⁻²)	<i>n</i>	<i>X</i> ²	<i>η</i>
0	222	59.4	0.834	0.003361	-
25	1153	53.2	0.820	0.005392	80.7
50	1490	47.8	0.816	0.004842	85.1
75	2290	42.4	0.824	0.005901	90.3
100	2680	33.0	0.841	0.007123	91.7

Table 3. The values of the corrosion parameters obtained from potentiodynamic polarization curves for mild steel in 1.0 M HCl solution containing different concentrations of DPhDMA

Concentration(ppm)	<i>E</i> (mv)	<i>I_{corr}</i> (μA/cm ²)	<i>β_a</i> (mV/dec)	<i>β_c</i> (mV/dec)	<i>η</i>
0	-492	179.7	117	121	-
25	-493	42.6	128	117	76.3
50	-480	31.3	136	114	82.6
75	-478	24.3	135	116	86.5
100	-477	19.92	133	115	88.9

**Fig. 7.** Potentiodynamic polarization curves for mild steel obtained in 1.0 M HCl solution containing different concentrations of DPhDMA

upon the adsorption of inhibitor molecules substituting for smaller molecules and ions having higher dielectric coefficients (*K*) such as water and chloride, the electric double layer thickness (*d*) increases and hence the values of electric double layer capacitance decrease [30–32].

Besides, increasing the inhibitor concentration up to 100 ppm increases the number of the adsorbed molecules on the metal surface as well as the surface coverage of mild

steel specimens. Therefore, the inhibition efficiency of the investigated inhibitor increases from 80.7% at the presence of 25 ppm of this compound to 91.7 % at 100 ppm concentration of it.

3. 3. Potentiodynamic polarization tests

Fig 7 shows the potentiodynamic polarization curves for mild steel samples in 1.0 M HCl solution with and without the addition of different concentrations of the synthesized inhibitor. Polarization parameters such as the corrosion potential, anodic and cathodic Tafel slopes, corrosion current density and inhibition efficiency of the investigated inhibitor are listed in Table 3. Here, the inhibition efficiency is calculated using the following formula:

$$\eta = \left(1 - \frac{i_{inh}}{i_{uninh}}\right) \times 100 \quad [7]$$

Where *i_{inh}* and *i_{uninh}* are corrosion current densities of mild steel in 1.0 M HCl solution in the presence and absence of inhibitor, respectively.

It is obvious from Fig 7 that with the introduction of the investigated inhibitor to 1.0 M HCl solution and increasing its concentration, both anodic and cathodic

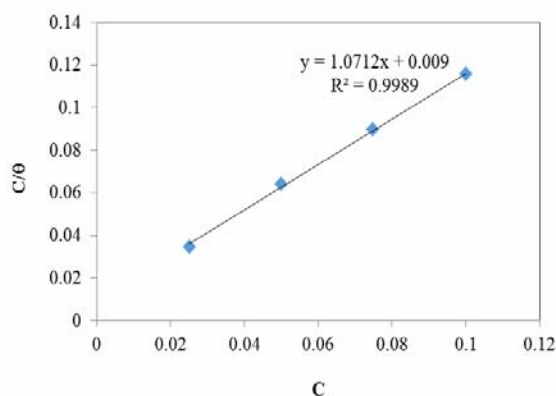


Fig. 8. Langmuir isotherm adsorption mode of DPhDMA on the mild steel surface

branches of polarization curves shift towards lower current densities, implying that the investigated compound acts as an effective mixed type inhibitor impeding both the hydrogen evolution and metal dissolution reactions [33, 34]. This is also confirmed by the values from Table 3. As can be seen, the value of corrosion current density decreases from $179.7 \mu\text{A}/\text{cm}^2$ in the absence of the inhibitor to $19.92 \mu\text{A}/\text{cm}^2$ in the presence of 100 ppm of this compound in the corrosive media and hence the inhibition efficiency of this compound increases with its concentration. Also, no monotonic trend can be observed for the change in the values of anodic and cathodic Tafel slopes which further attests to the mixed type inhibition effect of the investigated inhibitor [19].

Moreover, both cathodic and anodic current-potential curves give rise to parallel lines, indicating that the addition of DPhDMA to 1.0 M HCl solution does not modify neither the anodic dissolution of mild steel samples nor the hydrogen evolution mechanism at the mild steel surface which occur mainly through a charge transfer mechanism [35].

The inhibition effect of this inhibitor might be caused by the simple blocking effect, namely the reduction of active corroding sites of the surface and as a result, higher inhibitor concentrations lead to higher surface coverage of the inhibitor film on mild steel specimens and higher inhibition efficiency of this compound. Therefore, only the un-covered surface and the presence of defects on the mild steel specimens allow the access of H^+ ions to

the mild steel surface [36, 37].

3. 4. Adsorption isotherm and thermodynamic parameters

It is widely known that organic inhibitors act through physisorption or chemisorption or a combination of both on the metal surface. The correlation of θ obtained from weight loss, potentiodynamic polarization and EIS tests, with concentration of DPhDMA was evaluated using different adsorption isotherms such as Frankin, Langmuir, Temkin and Freundlich in order to obtain more information about the interaction between the inhibitor molecules and the metal surface and Langmuir adsorption isotherm was found to be the best fit [38, 39]:

$$\frac{c}{\theta} = c + \frac{1}{K_{\text{ads}}} \quad [8]$$

Where θ is the surface coverage of steel by DPhDMA molecules, C_i is the concentration of DPhDMA and K_{ads} is the adsorptive equilibrium constant.

Fig 8 describes the dependence of C/θ on the concentration of DPhDMA according to the results from weight loss tests. As can be seen, linear plot is obtained with slope very close to 1 denoting the monolayer adsorption of DPhDMA on the steel surface. Also, the deviation of slope from unity can be attributed to the adsorption of inhibitor on different sites of mild steel surface [40].

The adsorptive equilibrium constant is related to the standard free energy of adsorption (ΔG_{ads}^0) according to the following equation [41, 42]:

$$K_{\text{ads}} = \frac{1}{C_{\text{H}_2\text{O}}} \exp\left(\frac{-\Delta G_{\text{ads}}^0}{RT}\right) \quad [9]$$

Where R is the gas constant ($8.314 \text{ J mol}^{-1} \text{ K}^{-1}$), T is the absolute temperature (K), and the value $C_{\text{H}_2\text{O}}$ is the concentration of water in the solution expressed in molar equals to 1000 gL^{-1} .

It is well accepted that the values of ΔG_{ads}^0 up to -20 kJ mol^{-1} or less negative are consistent with electrostatic interaction between charged inhibitor molecules and charged metal surface (physical adsorption), while values more negative than -40 kJ mol^{-1} are associated with sharing or transferring of electrons from the inhibitor molecule to the metal surface to form

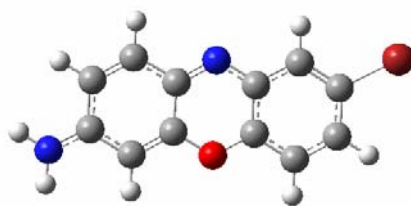


Fig. 9. Optimized molecular structure of DPhDMA

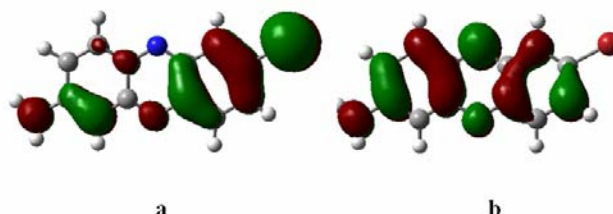


Fig. 10. Frontier molecular orbital density distributions of DPhDMA a) HOMO b) LUMO

Table 4. Quantum chemical parameters derived for DPhDMA

Compound	E_{HOMO} (eV)	E_{LUMO} (eV)	ΔE (eV)	μ (Debye)
DPhDMA	- 9.869	-7.264	2.604	12.85

a co-ordinate type of bond (chemisorption) [42, 43].

The ($\Delta G^{\circ}_{\text{ads}}$) was calculated as 28.78 kJ mol⁻¹. Considering the sign and value of the standard free energy of adsorption, it can be concluded that the adsorption of DPhDMA molecules on mild steel surface occurs spontaneously through a combination of physical and chemical adsorption.

3. 5. Quantum chemical calculations

The quantum chemical calculations were carried out to study the relationship between the molecular structure of DPhDMA molecule and its inhibition efficiency.

The optimized geometry of the DPhDMA is represented in Fig 9 and their corresponding frontier molecular orbitals density distributions, HOMO and LUMO, are presented in Figure 10a and 10b, respectively.

Fig 10 shows the distribution of the HOMO electron density which is strongly concentrated on ring 3 (from left), the Bromine atom and some Carbon atoms of ring 1 and endocyclic Oxygen, indicating that these sites might be the preferred active centers for the adsorption of the inhibitors on the metal surface. The aminic Nitrogen from ring 1 as a donor shares its

electron pair through resonance with π electron pairs of the rings number 1,2 and 3 and electron pair of endocyclic Oxygen from ring 2. Finally, the Bromine atom from ring 3 as an acceptor group has the highest electron density of all. Therefore, π electron pairs from rings along with electron pairs of the Bromine atom and endocyclic Oxygen act as active adsorption sites on the surface.

Some electronic properties of DPhDMA such as the energy of the highest occupied molecular orbital (E_{HOMO}), energy of the lowest unoccupied molecular orbital (E_{LUMO}), the energy band gap, ΔE ($E_{\text{LUMO}} - E_{\text{HOMO}}$), and dipole moment (μ) are reported in Table 4.

It has been reported that the higher the value of E_{HOMO} , the greater the ability of donating electron to unoccupied d orbital of the metal and hence the higher inhibition efficiency of the inhibitor under debate. Also, the lower the value of E_{LUMO} , the greater the tendency to accept electron from the metal surface as the energy gap decreased and the inhibition efficiency of the inhibitor increased [44, 45].

Some studies reported that higher dipole moments can lead to increase in inhibition efficiency which might be due to the dipole-dipole interactions of molecules and metal

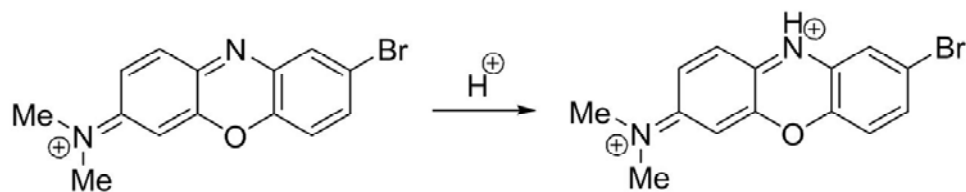


Fig. 11. Protonation mechanism of DPhDMA

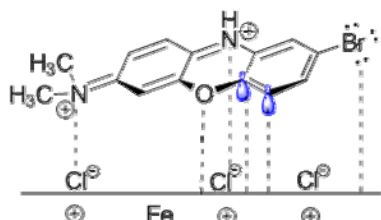


Fig. 12. Schematic mechanism of corrosion inhibition of DPhDMA

surface and easier electron transfer from inhibitor to the metal surface [46–48].

As can be seen from Table 4, the dipole moment value for DPhDMA molecule was found to be 12.850 Debye (42.85948×10^{-30} Cm), which was higher than that of H_2O (6.23×10^{-30} cm), indicating that the electron transfer to the surface occurs from DPhDMA molecules other than water molecules while DPhDMA molecules are substituting for them during adsorption on mild steel surface.

3. 6. Mechanism of corrosion inhibition

It is well recognized that organic molecules used as inhibitors mitigate the corrosion reactions through the adsorption on the metal. Organic molecules may be adsorbed on the metal surface in one or more of the following ways:

(1) Electrostatic interaction of protonated molecules with Cl^- ions that are already adsorbed on the surface (physisorption); (2) donor-acceptor interactions between the π -electrons of aromatic ring and vacant d orbital of surface iron atoms; (3) interaction between unshared electron pairs of oxygen atoms and vacant d-orbital of surface iron atoms (chemisorption) [49–51].

DPhDMA molecule can be protonated in acid medium as shown in fig 11.

It is believed that corrosion inhibitor molecules act using adsorption on the metal surface. Based on this, DPhDMA can be

adsorbed on the steel surface which is schematically shown in Fig 12. Electrostatic interactions of those atoms which have positive charge with adsorbed Cl^- ion on the steel surface is one of the adsorption ways. The second way is donor-acceptor interactions between iron vacant d-orbital and π -electrons of aromatic rings, and the third one is the interaction of unshared electrons of oxygen and bromine atoms with iron vacant d-orbital.

4. Conclusions

1. DPhDMA showed good inhibiting properties for mild steel in 1M HCl solution. Furthermore, the inhibition efficiency values increased with increasing the concentration of DPhDMA.
2. EIS curves exhibited that polarization resistance of the mild steel electrode increases while its capacitance decreases upon the introduction of DPhDMA to the corrosive solution.
3. Potentiodynamic polarization tests revealed that DPhDMA acts as an efficient combination of anodic and cathodic type inhibitor against mild steel corrosion in 1M HCl solution and its inhibition efficiency increases with its concentration.
4. DPhDMA acts through a combination of physical and chemical adsorption on mild steel surface which obeys the Langmuir adsorption isotherm.
5. Quantum chemical study revealed that π electron pairs from rings along with electron pairs of the Bromine atom and endocyclic Oxygen might be the active sites for adsorption onto the steel surface.

References

1. P. Bothi, A. Kaleem, A. Abdul, H. Osman, K. Awang, "Neolamarckia cadamba alkaloids as eco-friendly corrosion inhibitors for mild steel in

- 1 M HCl media”, *Corros. Sci.*, Vol. 69, 2013, pp. 292–301.
- E. M. Sherif, S. Park, “Effects of 2-Amino-5-Ethylthio-1, 3, 4-Thiadiazole on copper corrosion as a corrosion inhibitor in aerated acidic pickling solutions”, *Electrochim. Acta*, Vol. 51, 2006, pp. 6556–6562.
 - M. Znini, G. Cristofari, L. Majidi, A. Ansari, A. Bouyanzer, J. Paolini, J. Costa, B. Hammouti, “Green approach to corrosion inhibition of mild steel by essential oil leaves of asteriscus graveolens (Forssk .) in sulphuric acid medium”, *Int. J. Electrochem. Sci.*, Vol. 7, 2012, pp. 3959 – 3981.
 - H. B. Ouici, O. Benali, Y. Harek, L. Larabi, B. Hammouti, A. Guendouzi, “Inhibition of mild steel corrosion in 5 % HCl solution by 5-(2-Hydroxyphenyl)-1,2,4-Triazole-3-Thione”, *Res. Chem. Intermed.*, Vol. 39, 2013, pp. 2777–2793.
 - A. Kosari, M. H. Moayed, A. Davoodi, R. Parvizi, M. Momeni, H. Eshghi, H. Moradi, “Electrochemical and quantum chemical assessment of two organic compounds from pyridine derivatives as corrosion inhibitors for mild steel in HCl solution under stagnant condition and hydrodynamic flow”, *Corros. Sci.*, Vol. 78, 2014, pp. 138–150.
 - H. Cang, W. Shi, J. Shao, Q. Xu, “Study of stevia rebaudiana leaves as green corrosion inhibitor for mild steel in sulphuric acid by electrochemical techniques”, *Int. J. Electrochem. Sci.*, Vol. 7, 2012, pp. 3726–3736.
 - H. Gerengi, H. I. Sahin, “Schinopsis lorentzii extract as a green corrosion inhibitor for low carbon steel in 1 M HCl solution”, *Ind. Eng. Chem. Res.*, Vol. 51, 2012, pp. 780–787.
 - A. M. Al-Sabagh, M. A. Migahed, M. A. El-Raouf, “Corrosion inhibition of carbon steel during acid cleaning process by a new synthesized polyamide based on thiourea corrosion inhibition of carbon steel during acid cleaning process by a new synthesized polyamide based on thiourea”, *Chem. Eng. Comm.*, Vol. 199, 2012, pp. 737–750.
 - S. H. Kumar, S. Karthikeyan, “Torsemide and furosemide as green inhibitors for the corrosion of mild steel in hydrochloric acid medium”, *Ind. Eng. Chem. Res.*, Vol. 52, 2013, pp. 7457–7469.
 - S. John, A. Joseph, “Electro analytical, surface morphological and theoretical studies on the corrosion inhibition behavior of different 1, 2, 4-Triazole precursors on mild steel in 1 M hydrochloric acid”, *Mater. Chem. Phys.*, Vol. 133, 2012, pp. 1083–1091.
 - Y. Yan, W. Li, L. Cai, B. Hou, “Electrochemical and quantum chemical study of purines as corrosion inhibitors for mild steel in 1 M HCl solution”, *Electrochim. Acta*, Vol. 53, 2008, pp. 5953–5960.
 - M. G. Pavlovic, “Synergistic effect between nonionic surfactant and halide Ions in the forms of inorganic or organic salts for the corrosion inhibition of stainless-steel X4Cr13 in sulphuric acid”, *Corros. Sci.*, Vol. 58, 2012, pp. 192–201.
 - S. K. Shukla, A. K. Singh, M. A. Quraishi, “Triazines: Efficient corrosion inhibitors for mild steel in hydrochloric acid solution”, *Int. J. Electrochem. Sci.*, Vol. 7, 2012, pp. 3371–3389.
 - S. Hejazi, M. H. Moayed, M. Rahimizadeh, A. Eslami, M. Momeni, A. Shiri, “Inhibitive assessment of 1-(7-Methyl-5-Morpholin-4-Yl-Thiazolo [4, 5- D] Pyrimidin-2-Yl) -Hydrazine as a corrosion inhibitor for mild steel in sulfuric acid solution”, *J. Iran. Chem. Soc.*, Vol. 10, 2013, pp. 831–839.
 - N. Missoum, A. Guendouz, N. Boussalah, B. Hammouti, A. Chetouani, M. Taleb, A. Aouniti, S. Ghalem, “Synthesis and evaluation of bipyrazolic derivatives as inhibitors of corrosion of C38 steel in molar hydrochloric acid”, *Res. Chem. Intermed.*, Vol. 39, 2013, pp. 3441–3461.
 - N. A. Negm, E. A. Badr, I. A. Aiad, M. F. Zaki, M. M. Said, “Investigation the Inhibitory Action of Novel Diquaternary Schiff Dibases on the Acid Dissolution of Carbon Steel in 1 M Hydrochloric Acid Solution”, *Corros. Sci.*, Vol. 65, 2012, pp. 77–86.
 - M. Abdallah, B. H. Asghar, I. Zafarany, A. S. Fouda, “The inhibition of carbon steel corrosion in hydrochloric acid solution using some phenolic compounds”, *Int. J. Electrochem. Sci.*, Vol. 7, 2012, pp. 282 – 304.
 - Z. El Adnani, M. Mcharfi, M. Sfaira, A. T. Benjelloun, M.E. Touhami, “Investigation of newly pyridazine derivatives as corrosion inhibitors in molar hydrochloric acid. Part iii: Computational calculations”, *Int. J. Electrochem. Sci.*, Vol. 7, 2012, pp. 3982–3996.
 - M. A. Hegazy, A. M. Hasan, M. M. Emara, M. F. Bakr, A. H. Youssef, “Evaluating four synthesized schiff bases as corrosion inhibitors on the carbon steel in 1 M hydrochloric acid”, *Corros. Sci.*, Vol. 65, 2012, pp. 67–76.
 - D. Ben Hmamou, R. Salghi, A. Zarrrouk, M. R. Aouad, O. Benali, H. Zarrok, M. Mesali, B. Hammouti, E. Ebenso, M. M. Kabanda, M. Bouachrine, “Weight loss, electrochemical, quantum chemical calculations and molecular dynamics simulation studies on 2-(Benzylthio)-1,4,5-Triphenyl-1h-Imidazole as inhibitor for carbon steel corrosion in hydrochloric acid”, *Ind. Eng. Chem. Res.*, Vol. 52, 2013, pp. 14315–14327.

21. S. Ghareba, S. Omanovic, "12-Aminododecanoic acid as a corrosion inhibitor for carbon steel", *Electrochim. Acta*, Vol. 56, 2011, pp. 3890–3898.
22. E. M. Sherif, S. Arabia, "Corrosion inhibition in chloride solutions of iron By 3-Amino-1,2,4-Triazole-5-Thiol and 1,1'-Thiocarbonyldiimidazole", *Int. J. Electrochem. Sci.*, Vol. 7, 2012, pp. 4834–4846.
23. N. Ottawa, G. Schafer, "Process for the manufacture of basic oxazine dyestuffs", United States Patent Office, 1972.
24. K. W. Tan, M. J. Kassim, C. W. Oo, "Possible improvement of catechin as corrosion inhibitor in acidic medium", *Corros. Sci.*, Vol. 65, 2012, pp. 152–162.
25. S. Yoo, Y. Kim, K. Chung, N. Kim, J. Kim, "Corrosion inhibition properties of Triazine derivatives containing carboxylic acid and amine groups in 1.0 M HCl solution", *Ind. Eng. Chem. Res.*, Vol. 52, 2013, pp. 10880–10889.
26. P. Bommersbach, J. P. Millet, B. Normand, "Formation and behaviour study of an environment-friendly corrosion inhibitor by electrochemical methods", *Electrochim. Acta*, Vol. 51, 2005, pp. 1076–1084.
27. A. R. Hoseinzadeh, I. Danaee, M. H. Maddahy, M. Rashvandavei, "Taurine as a green corrosion inhibitor for Aisi 4130 steel alloy in hydrochloric acid solution", *Chem. Eng. Comm.*, Vol. 201 2014, pp. 380–402.
28. P. B. Raja, A. K. Qureshi, A. A. Rahim, H. Osman, K. Awang, "Neolamarckia cadamba alkaloids as eco-friendly corrosion inhibitors for mild steel in 1M HCl media", *Corros. Sci.*, Vol. 60, 2009, pp. 289–296.
29. X. Li, S. Deng, "Inhibition effect of dendrocalamus brandisii leaves extract on aluminum in HCl, H₃PO₄ Solutions", *Corros. Sci.*, Vol. 65, 2012, pp. 299–308.
30. K. Cao, W. Li, L. Yu, "Investigation of 1-Phenyl-3-Methyl-5-Pyrazolone as a corrosion inhibitor for mild steel in 1M hydrochloric acid", *Int. J. Electrochem. Sci.*, Vol. 7, 2012, pp. 806–818.
31. A. E. O. Yüce, R. Solmaz, G. Kardas, "Investigation of inhibition effect of rhodanine-N-acetic acid on mild steel corrosion in HCl solution", *Mater. Chem. Phys.*, Vol. 131, 2012, pp. 615–620.
32. M. Elbakri, R. Tourir, M. E. Touhami, A. Zarrouk, Y. Aouine, M. Sfaira, M. Bouachrine, A. Alami, A. El Hallaoui, "Inhibiting effects of benzamide derivatives on the corrosion of mild steel in hydrochloric acid solution", *Res. Chem. Intermed.*, Vol. 39, 2013, pp. 2417–2433.
33. W. Qafsaoui, M. W. Kendig, H. Perrot, H. Takenouti, "Coupling of electrochemical techniques to study copper corrosion inhibition in 0.5 Mol L⁻¹ NaCl by 1-Pyrrolidine Dithiocarbamate", *Electrochim. Acta*, Vol. 87, 2013, pp. 348–360.
34. S. Kumar, D. Sharma, P. Yadav, M. Yadav, "Experimental and quantum chemical studies on corrosion inhibition effect of synthesized organic compounds on N80 steel in hydrochloric acid", *Ind. Eng. Chem. Res.*, Vol. 52, 2013, pp. 14019–14029.
35. B. Duran, A. Yurt, "Schiff bases as corrosion inhibitor for aluminum in HCl solution", *Corros. Sci.*, Vol. 54, 2012, pp. 251–259.
36. L. Li, Q. Qu, W. Bai, F. Yang, Y. Chen, S. Zhang, Z. Ding, "Sodium Diethyldithiocarbamate as a corrosion inhibitor of cold rolled steel in 0.5 M hydrochloric acid solution", *Corros. Sci.*, Vol. 59, 2012, pp. 249–257.
37. F. Zhang, J. Pan, P. M. Claesson, "Electrochemical and AFM studies of mussel adhesive protein (Mefp-1) as corrosion inhibitor for carbon steel", *Electrochim. Acta*, Vol. 56, 2011, pp. 1636–1645.
38. M. Bozorg, T. Shahrabi Farahani, J. Neshati, Z. Chaghazardi, G. Mohammadi Ziarani, "Myrtus communis as green inhibitor of copper corrosion in sulfuric acid", *Ind. Eng. Chem. Res.*, Vol. 53, 2014, pp. 4295–4303.
39. B. Xu, W. Yang, Y. Liu, X. Yin, W. Gong, Y. Chen, "Experimental and theoretical evaluation of two Pyridinecarboxaldehyde Thiosemicarbazone compounds as corrosion inhibitors for Mild Steel in Hydrochloric Acid Solution", *Corros. Sci.*, Vol. 78, 2014, pp. 260–268.
40. E. S. Meresht, T. S. Farahani, J. Neshati, "2-Butyne-1, 4-Diol as a novel corrosion inhibitor for Api X65 Steel pipeline in carbonate/bicarbonate solution", *Corros. Sci.*, Vol. 54, 2012, pp. 36–44.
41. B. Xu, W. Yang, Y. Liu, X. Yin, W. Gong, Y. Chen, "Experimental and theoretical evaluation of two pyridinecarboxaldehyde thiosemicarbazone compounds as corrosion inhibitors for mild steel in hydrochloric acid solution", *Corros. Sci.*, Vol. 78, 2014, pp. 260–268.
42. A. Zarrouk, B. Hammouti, A. Dafali, F. Bentiss, M. Oujda, "Inhibitive properties and adsorption of purpald as a corrosion inhibitor for copper in nitric acid medium", *Ind. Eng. Chem. Res.*, Vol. 52, 2013, pp. 2560–2568.
43. G. Quartarone, L. Ronchin, A. Vavasori, C. Tortato, L. Bonaldo, "Inhibitive action of gramine towards corrosion of mild steel in deaerated 1.0 M hydrochloric acid solutions",

- Corros. Sci., Vol. 64, 2012, pp. 82–89.
44. C. M. Goulart, A. Esteves-Souza, C. A. Martinez-Huitle, C. J. F. Rodrigues, M. A. M. Maciel, A. Echevarria, “Experimental and theoretical evaluation of semicarbazones and thiosemicarbazones as organic corrosion inhibitors”, *Corros. Sci.*, Vol. 67, 2013, pp. 281–291.
45. N. S. Patel, S. Jauhari, G. N. Mehta, B. Hammouti, M. Bouachrine, “The effect of 2-aminoquinoline-6-Carboxylic acid on the corrosion behavior of mild steel in hydrochloric acid”, *J. Iran. Chem. Soc.*, Vol. 9, 2012, pp. 635–641.
46. M. A. Hegazy, A. M. Badawi, S. S. A. El, W. M. Kamel, “Corrosion inhibition of carbon steel using novel N-(2-(2-Mercaptoacetoxy)Ethyl)-N,N-Dimethyl Dodecan-1-Aminium Bromide during acid pickling”, *Corros. Sci.*, Vol. 69, 2013, pp. 110–122.
47. N. O. Obi-Egbedi, I. B. Obot, “Inhibitive Properties , Thermodynamic and quantum chemical studies of alloxazine on mild steel corrosion in H₂SO₄”, *Corros. Sci.*, Vol. 53, 2011, pp. 263–275.
48. I. B. Obot, N. O. Obi-Egbedi, A. O. Eseola, “Phenanthroline on mild steel in sulfuric acid solution□: Experimental and theoretical study”, *Ind. Eng. Chem. Res.*, Vol. 50, 2011, pp. 2098–2110.
49. I. Ahamad, R. Prasad, E. E. Ebenso, M. A. Quraishi, “Electrochemical and quantum chemical study of albendazole as corrosion inhibitor for mild steel in hydrochloric acid solution”, *Int. J. Electrochem. Sci.*, Vol. 7, 2012, pp. 3436 – 3452.
50. N. A. Negm, N. G. Kandile, E. A. Badr, M. A. Mohammed, “Gravimetric and electrochemical evaluation of environmentally friendly nonionic corrosion inhibitors for carbon steel in 1M HCl”, *Corros. Sci.*, Vol. 65, 2012, pp. 94–103.
51. A. Singh, I. Ahamad, D. K. Yadav, V. K. Singh, “The effect of environmentally benign fruit extract of shahjan (Moringa Oleifera) on the corrosion of mild steel in hydrochloric acid solution”, *Chem. Eng. Comm.*, Vol. 199, 2011, pp. 37–41.